

A Complex Impedance-Transforming Coupled-Line Balun

Weiwei Zhang^{1, *}, Yuanan Liu¹, Yongle Wu^{1, 2},
Weimin Wang¹, Ming Su¹, and Jinchun Gao¹

Abstract—An asymmetrical coupled-line circuit is proposed to design a planar microstrip balun, which has the advantages of compact structure and complex source to complex load impedance transformation. This balun consists of three pairs of coupled lines and two tapped transmission-line stubs. Based on the traditional even-odd mode technique and $ABCD$ parameters, closed-form mathematical equations for circuit electrical parameters are obtained. To demonstrate our design theory, a practical microstrip balun is designed, simulated and measured. The results show that the return loss is larger than 25 dB, the insertion loss S_{21} (S_{31}) 3.15 dB (3.29 dB), and the output phase difference -180.22° at the operating frequency. Good agreements between the simulated and measured results verify our design theory.

1. INTRODUCTION

Balun is an important component in the wireless communication systems to transform the unbalanced input signal into two output balanced signals and vice versa. It can be used in mixers, balanced antennas, push-pull amplifiers, etc. Among the existing planar balun circuits, the power-divider and phase shifter based balun [1], Marchand balun [2], and branch-line balun [3–6] are very popular due to their easy realization and low cost. A broad-band balun composed of a Wilkinson power divider and a wide-band 180° phase shifter is described in [1]. Two identical coupled lines are used to design an impedance-transforming Marchand balun which cannot be realized through the planar microstrip coupled line because of its tight coefficient limitation [2]. Since the basic 3-port balun theory can be derived from the symmetrical 4-port networks when one of the ports is open or short [3], many branch-line baluns, including impedance transforming balun [4] based on the branch line structure, dual-band balun [5] using the tapped stepped impedance, size-reduction balun [6] meandering the branches and attaching a stub, have been researched.

However, only the real source and load impedances are considered in almost all the baluns. For general microwave circuits, complex impedances are usually needed in the active circuits and systems. Unfortunately, the planar balun with complex impedances is still blank.

Therefore, this paper mainly describes a planar microstrip balun with inherent complex source to complex load terminated impedances. By using the traditional even-odd mode analysis and $ABCD$ parameters, closed-form equations about the circuit parameters are obtained in Section 2. An experimental balun operating at 2 GHz is designed, simulated, and measured in Section 3. A conclusion is given at last.

Received 24 June 2014, Accepted 1 September 2014, Scheduled 5 September 2014

* Corresponding author: Weiwei Zhang (clarence.zhang11@gmail.com).

¹ Beijing Key Laboratory of Work Safety Intelligent Monitoring, Beijing University of Posts and Telecommunications, Beijing, China.

² State Key Laboratory of Millimeter Waves, Southeast University, Nanjing 210096, China.

2. CIRCUIT STRUCTURE AND DESIGN THEORY

Figure 1 shows the structure of the proposed coupled-line balun. This proposed complex impedance-transforming balun has the source impedance $R_S + jX_S$ and load impedance $R_L + jX_L$. It consists of three pairs of coupled lines and two tapped transmission-line stubs. The even-mode characteristic impedance of the first (second, and third) coupled line is Z_{e1} (Z_{e2} , and Z_{e3}), and the odd-mode impedance is Z_{o1} (Z_{o2} , and Z_{o3}). The electrical lengths of these three coupled lines are θ_1 , θ_2 , and θ_3 , respectively. The two tapped stubs, which are used to realize short circuits under the even-mode excitation, have characteristic impedances with Z_4 (Z_5) and electrical lengths with θ_4 (θ_5). Note that all the electrical lengths can be selected from 0° to 90° . This balun can also be seen as a symmetrical 4-port circuit whose one port is open.

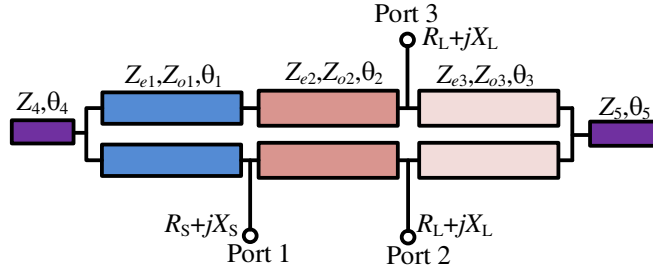


Figure 1. The circuit structure of the proposed coupled-line balun with complex impedance-transformation.

In order to obtain the closed-form solution, even- and odd-mode methods are used [6]. The equivalent even- and odd-mode transmission line circuits of the proposed balun are shown in Fig. 2. The sufficient conditions for the balun are as follows:

$$T_{even} = 0, \quad (1a)$$

$$S_{11e} + S_{11o} - 2S_{11e}S_{11o} = 0. \quad (1b)$$

where T_{even} is the transmission coefficient under the even mode at the port 1, and S_{11e} (S_{11o}) is the reflected coefficient under the even (odd) mode at the port 1.

2.1. Even-Mode Analysis

In the even mode, a magnetic wall is formed along the symmetric line. The tapped stub Z_4 (Z_5) can be split into two parallel stubs $2Z_4$ ($2Z_5$), and their electrical lengths remain the same, as shown in Fig. 2(a). Since a $\lambda/4$ open stub can satisfy Equation (1a) and produce a transmission zero at the operating frequency, the following equations can be adopted:

$$Z_4 = 0.5Z_{e1}, \quad (2a)$$

$$Z_5 = 0.5Z_{e3}, \quad (2b)$$

$$\theta_4 = 90^\circ - \theta_1, \quad (2c)$$

$$\theta_5 = 90^\circ - \theta_3. \quad (2d)$$

Since port 1 is shorted at Equation (2), the reflected coefficient S_{11e} at the operating frequency can be calculated as

$$S_{11e} = \frac{jX_S - R_S}{jX_S + R_S}, \quad (3)$$

where the subscript e denotes the even mode.

2.2. Odd-Mode Analysis

In the odd mode, an electric wall is formed along the symmetric line. The tapped stubs Z_4 (Z_5) are shorted by the virtual ground, as shown in Fig. 2(b). To simplify the analytical process, the electrical length $\theta_2 = 90^\circ$ can be chosen.

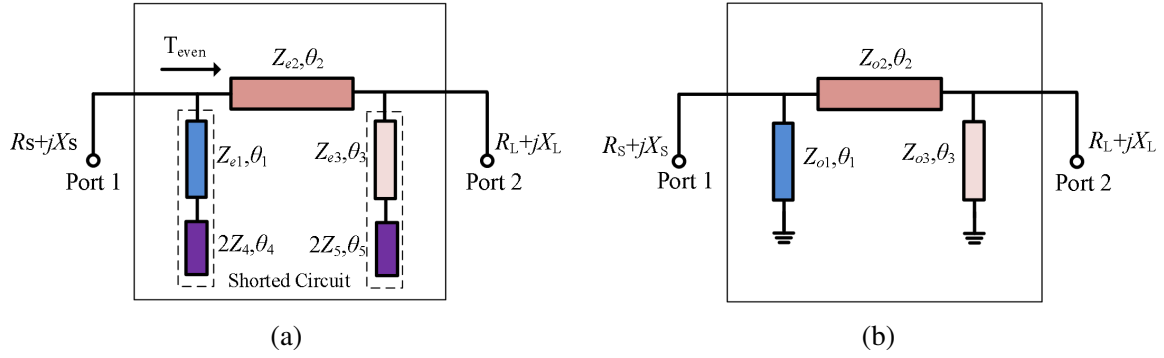


Figure 2. (a) Even-mode, (b) odd-mode equivalent circuits of the proposed coupled-line balun.

The reflected coefficient S_{11o} can be found in [7]:

$$S_{11o} = \frac{A_o(R_L + jX_L) + B_o - C_o(R_S - jX_S)(R_L + jX_L) - D_o(R_S - jX_S)}{A_o(R_L + jX_L) + B_o + C_o(R_S + jX_S)(R_L + jX_L) + D_o(R_S + jX_S)}, \quad (4)$$

where the subscript o denotes the odd mode. The $ABCD$ parameters of the odd-mode equivalent circuit in Fig. 2(b) are:

$$\begin{bmatrix} A_o & B_o \\ C_o & D_o \end{bmatrix} = \begin{bmatrix} 1 & 0 \\ \frac{1}{jZ_{o1} \tan \theta_1} & 1 \end{bmatrix} \begin{bmatrix} 0 & jZ_{o2} \\ \frac{1}{jZ_{o2}} & 0 \end{bmatrix} \begin{bmatrix} 1 & 0 \\ \frac{1}{jZ_{o3} \tan \theta_3} & 1 \end{bmatrix} = \begin{bmatrix} \frac{Z_{o2}}{Z_{o1} \tan \theta_1} & jZ_{o2} \\ \frac{j}{Z_{o2}} - \frac{Z_{o2}}{Z_{o1} Z_{o3} \tan \theta_1 \tan \theta_3} & \frac{Z_{o2}}{Z_{o1} \tan \theta_1} \end{bmatrix}. \quad (5)$$

After substituting Equations (3)–(5) into Equation (1b), the real and imaginary parts can be written separately as

$$\frac{R_S R_L Z_{o2}}{Z_{o3} \tan \theta_3} + \left(\frac{Z_{o2}}{Z_{o1} Z_{o3} \tan \theta_1 \tan \theta_3} - \frac{1}{Z_{o2}} \right) (2R_S X_S R_L - 2R_S^2 X_L) - \frac{2R_S^2 Z_{o2}}{Z_{o1} \tan \theta_1} = 0, \quad (6a)$$

$$\frac{R_S X_L Z_{o2}}{Z_{o3} \tan \theta_3} + Z_{o2} R_S - R_S (2X_S X_L + 2R_S R_L) \left(\frac{1}{Z_{o2}} - \frac{Z_{o2}}{Z_{o1} Z_{o3} \tan \theta_1 \tan \theta_3} \right) + \frac{2R_S X_S Z_{o2}}{Z_{o1} \tan \theta_1} = 0. \quad (6b)$$

Assuming that the parameters R_S , X_S , R_L , X_L , θ_1 , θ_3 , and Z_{o3} are known coefficients and then solving Z_{o1} and Z_{o2} simultaneously from Equation (6), we can obtain

$$Z_{o1} = \frac{2(R_L R_S^2 Z_{o3} \cot \theta_1 + R_L X_S^2 Z_{o3} \cot \theta_1)}{R_S X_L Z_{o3} - R_L X_S Z_{o3} + R_L^2 R_S \cot \theta_3 + R_S X_L^2 \cot \theta_3}, \quad (7a)$$

$$Z_{o2} = \frac{Z_{o3} \sqrt{2R_L (R_S^2 + X_S^2)}}{\sqrt{R_S Z_{o3}^2 + 2R_S X_L Z_{o3} \cot \theta_3 + R_S R_L^2 \cot^2 \theta_3 + R_S X_L^2 \cot^2 \theta_3}}. \quad (7b)$$

2.3. The Determination of Other Parameters

Generally, the realization of the coupled line is limited by the practical range of the coupling coefficients. We can define the relationships between the even-mode impedance and the odd-mode impedance as follows:

$$Z_{ei} = gZ_{oi}. \quad (i = 1, 2, \text{ and } 3) \quad (8)$$

Note that an appropriate value can be chosen for ratio g to make sure that the slot between the coupled lines is larger than 0.1 mm. Here, 1.2 can be selected for parameter g .

In practice, the fabrication of the microstrip circuits is limited by the range of realizable impedance from 20 Ω to 130 Ω , which can be described as:

$$20 \Omega < Z_{ei} < 130 \Omega. \quad (i = 1, 2, \text{ and } 3) \quad (9a)$$

$$20 \Omega < Z_{oi} < 130 \Omega. \quad (i = 1, 2, \text{ and } 3) \quad (9b)$$

$$20 \Omega < Z_i < 130 \Omega. \quad (i = 4, \text{ and } 5) \quad (9c)$$

2.4. The Design Procedure

Based on the investigations about the complex balun theory, the simple design procedure can be summarized as follows to make the design procedure easier.

- (1) Determine the operating frequency f_0 , the dielectric constant and thickness of the substrate material, and the complex source (load) impedance $R_S + jX_S$ ($R_L + jX_L$).
- (2) Choose the electrical lengths θ_1 and θ_3 , ($0^\circ < \theta_1, \theta_3 < 90^\circ$). Note that the electrical length θ_2 is 90° . Choose an appropriate odd-mode impedance Z_{o3} .
- (3) Use Equation (7) to calculate the odd-mode impedances of the coupled lines Z_{o1} , and Z_{o2} .
- (4) Obtain the even-mode impedances Z_{e1} , Z_{e2} , and Z_{e3} of the coupled-lines from Equation (8).
- (5) Substitute the parameters Z_{e1} , Z_{e3} , θ_1 , and θ_3 into Equation (2) to get parameters Z_4 , Z_5 , θ_4 , and θ_5 of the tapped subs. Note that all the impedances should satisfy Equation (9).
- (6) Convert the design parameters into physical dimensions by using the software of Advanced Design System (ADS).

3. SIMULATED AND MEASURED RESULTS

The analytical solutions and design procedures have been discussed in Section 2. In order to verify our proposed balun, an example is designed, simulated and measured. The microstrip balun, which operates at 2 GHz, is fabricated on F4B substrate with a dielectric constant of 2.65 and a thickness of 1 mm. The complex impedances of the input port $(40 - j10) \Omega$ and output port $(100 + j60) \Omega$ are chosen. In order to be measured by the Vector Network Analyzer directly, three transmission-line transformers are adopted between the three ports and the coupled-line balun because the source and load impedances are not 50Ω . The impedance Z_6 , which is between the port 1 and the balun, is 38.73Ω , and its electrical length is 37.76° . The impedance Z_7 , which is between the port 2 (3) and the balun, is 92.74Ω , and its electrical length is 57.10° . The top view of the fabricated balun is shown in Fig. 3. The circuit parameters are calculated as follows: $Z_{e1} = 78.07 \Omega$, $Z_{o1} = 65.05 \Omega$, $\theta_1 = 40^\circ$, $Z_{e2} = 78.39 \Omega$, $Z_{o2} = 65.33 \Omega$, $\theta_2 = 90^\circ$, $Z_{e3} = 84 \Omega$, $Z_{o3} = 70 \Omega$, $\theta_3 = 70^\circ$, $Z_4 = 39.03 \Omega$, $\theta_4 = 50^\circ$, $Z_5 = 42 \Omega$, $\theta_5 = 20^\circ$.

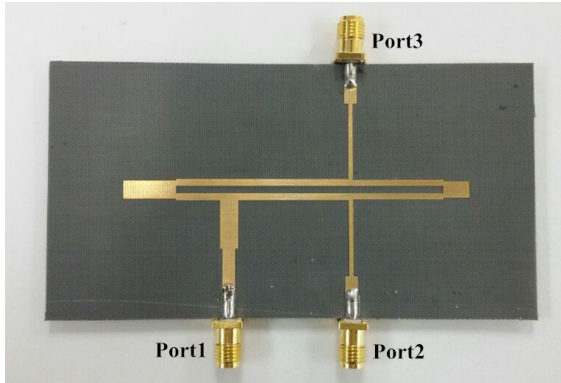


Figure 3. Top view of the fabricated coupled-line balun operating at $f_0 = 2$ GHz.

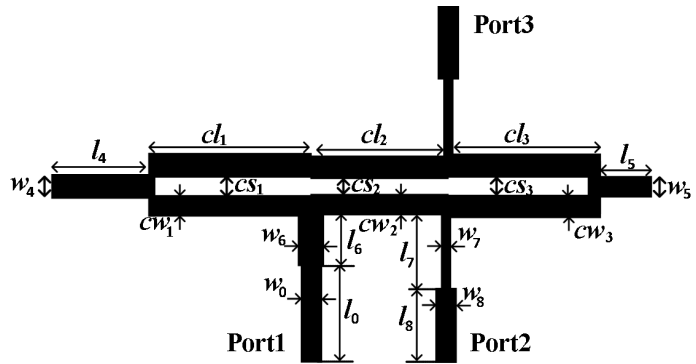


Figure 4. Layout of the proposed balun operating at $f_0 = 2$ GHz.

The layout of the proposed balun with defined dimensions is shown in Fig. 4. The physical circuit parameters are (unit: mm): $cw_1 = 1.50$, $cs_1 = 1.60$, $cl_1 = 11.25$, $cw_2 = 1.47$, $cs_2 = 1.60$, $cl_2 = 26.50$, $cw_3 = 1.32$, $cs_3 = 1.63$, $cl_3 = 19.80$, $w_0 = 2.74$, $l_0 = 14.50$, $w_4 = 3.91$, $l_4 = 11.25$, $w_5 = 3.56$, $l_5 = 5.56$, $w_6 = 3.96$, $l_6 = 10.52$, $w_7 = 0.91$, $l_7 = 16.43$, $w_8 = 2.74$, and $l_8 = 9.02$.

The proposed balun is simulated by HFSS and measured by the Vector Network Analyzer N5230C. The simulated and measured results agree very well as shown in Fig. 5. The reflected coefficient S_{11} is lower than -25 dB at both the simulated and measured results, showing that it has good return loss at the operating frequency. When the return loss at the port 1 is larger than 10 dB, the simulated (measured) operating bandwidth of the balun is from 1.78 to 2.32 GHz (1.85 to 2.23 GHz).

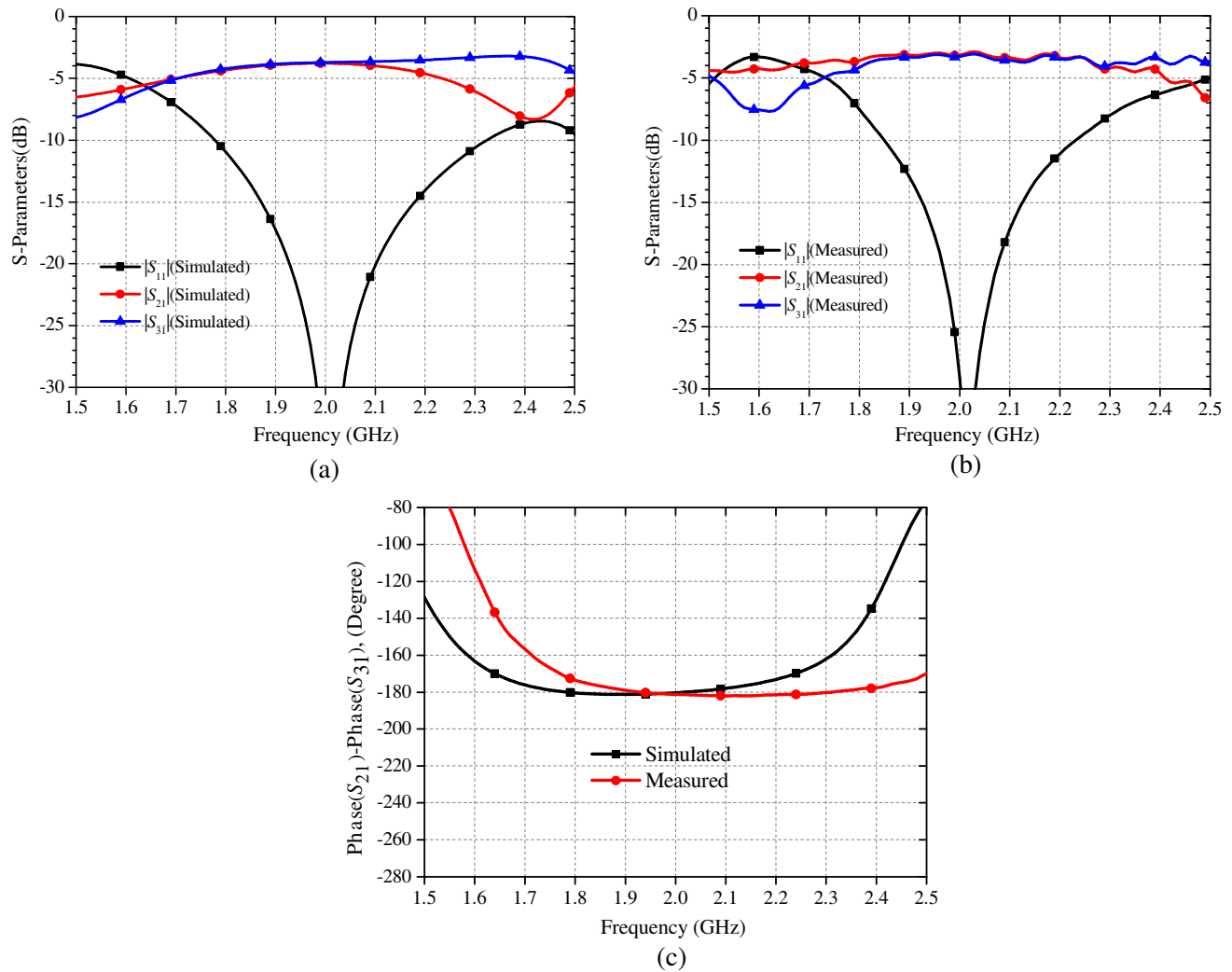


Figure 5. (a) Simulated scattering parameters. (b) Measured scattering parameters. (c) Phase difference between the two output ports of the proposed balun.

The measured results of the balun in Fig. 5(b) show that the insertion loss $|S_{21}|$ ($|S_{31}|$) has the amplitude balance from 2 dB to 4 dB in a wide frequency range from 1.67 (1.81) GHz to 2.26 (2.27) GHz. The insertion loss S_{21} (S_{31}) is 3.15 dB (3.29 dB) at the operating frequency, indicating that the magnitudes of the output signal are equal. The phase difference between port 2 and port 3 is -181.22° in Fig. 5(c). Table 1 lists the available bandwidth of the simulated and measured results to see the results clearly. Small performance degradation could be due to the dielectric losses, fabrication errors, or measurement errors, etc. It can be concluded that there is a good agreement between the simulated and measured results.

Table 1. The available bandwidth (GHz) of the simulated and measured results.

	BandWidth of S_{11} (< -10 dB)	BandWidth of S_{21} (± 1 dB)	BandWidth of S_{31} (± 1 dB)	BandWidth of Phase Difference ($\pm 5^\circ$)
Simulated	1.78–2.32	1.88–2.10	1.85–2.47	1.69–2.16
Measured	1.85–2.23	1.67–2.26	1.81–2.47	1.83–2.44

4. CONCLUSION

A planar microstrip coupled-line balun is proposed in this paper. This proposed balun, constructed by three pairs of coupled lines and two tapped stubs, features the compact structure and complex source to complex load impedance transformation. It can operate with good return loss, perfect amplitude performance and phase balance. Closed-form circuit analyses, analytical expressions, and the design procedures are given in Section 2. To demonstrate the practical balance performance, a typical microstrip balun is designed, fabricated, and measured. Good agreements between the simulated and measured results show that the proposed complex impedance-transforming balun will be very useful in the active circuits and systems.

ACKNOWLEDGMENT

This work was supported by the National Basic Research Program of China (973 Program) (No. 2014CB339900), National Science and Technology Major Project (No. 2012ZX03001001-002), National Natural Science Foundation of China (No. 61201027), National Natural Science Foundation of China for the Major Equipment Development (No. 61327806), Open Project of the State Key Laboratory of Millimeter Waves (Grant No. K201316), and Specialized Research Fund for the Doctor Program of Higher Education (No. 20120005120006).

REFERENCES

1. Zhang, Z.-Y., Y.-X. Guo, L. C. Ong, and M. Y. W. Chia, "A new wide-band planar balun on a single-layer PCB," *IEEE Microw. Wireless Compon. Lett.*, Vol. 15, No. 6, 416–418, Jun. 2005.
2. Ang, K. S. and I. D. Robertson, "Analysis and design of impedance-transforming planar Marchand baluns," *IEEE Trans. Microw. Theory Tech.*, Vol. 49, No. 2, 402–406, Feb. 2001.
3. Leong, Y. C., K. S. Ang, and C. H. Lee, "A derivation of a class of 3-port baluns from symmetrical 4-port networks," *IEEE MTT-S Int. Microwave Symp. Dig.*, Vol. 2, 1165–1168, Seattle, WA, United States, Jun. 2002.
4. Park, M.-J. and B. Lee, "Stubbed branch line balun," *IEEE Microw. Wireless Compon. Lett.*, Vol. 17, No. 3, 169–171, Mar. 2007.
5. Zhang, H., Y. Peng, and H. Xin, "A tapped stepped-impedance balun with dual-band operations," *IEEE Antennas Wirel. Propag. Lett.*, Vol. 7, 119–122, 2008.
6. Li, J.-L., S.-W. Qu, and Q. Xue, "Miniaturised branch-line balun with bandwidth enhancement," *Electron. Lett.*, Vol. 43, No. 17, 931–932, Aug. 2007.
7. Ahn, H.-R. and B. Kim, "Toward integrated circuit size reduction," *IEEE Microwave Mag.*, Vol. 9, No. 1, 65–75, Feb. 2008.